Research Article | Vol. 27, No. 22 / 28 October 2019 / Optics Express 32111
Optics EXPRESS

Phase-sensitive amplification of an optical field using microwaves

ASHA KARIGOWDA,[1,2,5] ADWAITH K V,[1,5] PRADOSH K. NAYAK,[1] S. SUDHA,[2] BARRY C. SANDERS,[1,3] FABIEN BRETENAKER,[1,4] AND ANDAL NARAYANAN[1,*]

[1]*Light and Matter Physics Group, Raman Research Institute, Bangalore 560080, India*
[2]*Department of Physics, Kuvempu University, Shankaraghatta, Shivamogga 577451, India*
[3]*Institute for Quantum Science and Technology, University of Calgary, Alberta, T2N 1N4, Canada*
[4]*Laboratoire Aimé Cotton, CNRS, Université Paris-Sud, ENS Paris-Saclay, Université Paris-Saclay, 91405 Orsay Cedex, France*
[5]*These two authors contributed equally*
[*]*andal@rri.res.in*

Abstract: We report phase-sensitive amplification (PSA) of a near-infrared electromagnetic field using room-temperature ^{85}Rb atoms possessing ground-state coherence. Our novelty is in achieving significant optical PSA by manipulating the intensity and phase of a frequency-separated microwave field. PSA is obtained by inducing a three-wave mixing nonlinear process utilising a three-level cyclic scheme in the D1 manifold. We achieve a near-ideal PSA with a gain of 7 dB over a range of 500 kHz bandwidth with very low pump-field intensities and with low optical depths. Such a hybrid, ground-state-coherence-assisted PSA is the first such demonstration using atomic ensembles.

1. Introduction

Frequency conversion of electromagnetic waves through nonlinear parametric processes can also be accompanied by amplification at a selected frequency [1–4]. After the discovery of coherent population trapping (CPT) phenomena [5–7] and the associated electromagnetically induced transparency (EIT) effect [8,9], gaseous alkali atoms have been increasingly used to achieve nonlinear amplification of weak signals [10–12]. This is because CPT shelves the atom in a dark state thereby eliminating its linear response to incident electromagnetic (EM) fields. This shelving enables the EM fields to interact with the atom nonlinearly even at moderate field intensities [11].

A phase-sensitive amplification (PSA) device is a phase-sensitive amplifier that amplifies a selected quadrature of an input electromagnetic field and de-amplifies its orthogonal quadrature [13]. Optical communication can improve significantly by PSA. A particular useful feature of a phase-sensitive amplifier is that, under ideal circumstances, the signal-to-noise ratio (SNR) of the input signal and output amplified signal remains unchanged. Such a feature enables specified quadrature amplification of signals without adding additional noise and thus PSA produced with nonlinear crystals has been used to demonstrate quantum non-demolition measurements [14]. In atomic systems, PSA has been demonstrated and exploited to improve two-mode quantum correlations [15]. Current phase-sensitive optical amplifiers operate within an all-optical domain requiring stringent conditions to maintain phase-matching and suffer from band-width loss allotted for idler fields. In cavity opto-mechanical systems, directional PSAs operating between microwave and optical photons have been recently proposed [16] but yet to be experimentally realized.

In atomic vapours, four-wave mixing ($\chi^{(3)}$) nonlinear electric-dipole response has been the symmetry-allowed lowest-order interaction exploited in experiments done until now to achieve

#373674 https://doi.org/10.1364/OE.27.032111
Journal © 2019 Received 24 Jul 2019; revised 27 Sep 2019; accepted 30 Sep 2019; published 21 Oct 2019

Optics EXPRESS

amplification. A nonlinear process in atomic vapours is efficient only if the atoms interacting with EM fields are prepared in a dark state, which eliminates linear response. Several interesting effects such as frequency conversion [17], squeezing of a noise quadrature [18] and indeed PSA [19] have all been demonstrated using atoms in a dark state. Recently we have shown that a three-wave mixing nonlinear response can be induced in atomic systems that are shelved in a dark state [20]. The dark state is prepared by ensuring that, one of the EM field interactions with the atom is a magnetic-dipole interaction. The magnetic-dipole interaction breaks the symmetry requirement and enables a three-wave mixing response to emerge in the centro-symmetric atomic system.

Exploiting this three-wave mixing interaction in ^{85}Rb atoms at room temperature, we demonstrate in this paper for the first time that significant amplification is achieved for an EM field. This amplification is phase-sensitive and coherent. Importantly we show that the PSA observed in the optical field can be controlled by the tunable intensity and phase of a frequency-separated microwave field. This effect was not shown before in any architecture that demonstrates PSA.

We show that our PSA's performance achieves the near-ideal limit, which implies that the amplification process adds very little noise to the signal. Such an ideal amplification, resulting from a PSA process, also signifies the presence of squeezing in the associated noise quadrature [13,19]. Low optical-field intensities and relatively low optical depths of our atomic ensemble makes our CPT-based PSA a very promising architecture to transfer and amplify quantum signals across different frequency domains.

2. Methods

We use a three-level Λ configuration of hyper-fine energy levels based on the D1 manifold of ^{85}Rb atoms. These levels are cyclically connected by three electromagnetic fields as shown in Fig. 1. This system is commonly referred to as a Δ (closed-Λ) system [21]. The coupling field is derived directly from an external cavity diode laser operating at 795 nm and which has a typical line-width of few hundred kHz. This addresses the transition connecting the meta-stable ground state $5^2S_{1/2}$, $F = 3$ ($|2\rangle$) and excited state $5^2P_{1/2}$, $F = 3'$ ($|3\rangle$) with a Rabi frequency Ω_c. The lower hyper-fine ground state $5^2S_{1/2}$, $F = 2$ ($|1\rangle$) and the excited state $5^2P_{1/2}$, $F = 3'$ ($|3\rangle$) transition is addressed by the probe beam with Rabi frequency Ω_p.

The probe beam is provided by phase modulating the coupling beam using an Electro-Optic Modulator (EOM) driven by a microwave source. A standing microwave field formed in a microwave cavity induces a magnetic dipole transition connecting the ground hyper-fine states $|1\rangle$ and $|2\rangle$ with a Rabi frequency Ω_μ. The coupling and probe optical fields and the standing microwave field together form a closed-Λ configuration. As the magnetic-dipole transition is weak, enriched ^{85}Rb atoms held in a 1 cm long vapor cell are placed inside a cylindrical microwave cavity supporting a TE_{011} mode. The measured quality factor (Q) of the loaded cavity with the cell falls within a range 10000 ± 1000 at 3.0357 GHz. The coupling and probe fields have typical powers of 75 μW and 15 μW respectively with a beam radius of 0.5 mm inside the vapor cell. All our results are obtained with an optical depth of 0.45 of our atomic sample.

Amplification in the probe field with a Δ system configuration of energy levels and electromagnetic fields is possible under two-photon and three-photon resonance conditions even with a room temperature [22] sample of ^{85}Rb atoms. In the context of nonlinear interactions amongst the applied fields, a three-photon resonance condition $\delta_p - \delta_c - \delta_\mu = 0$ is a statement of energy conservation. Here δ_p, δ_c and δ_μ, respectively, are the detunings of the probe, coupling and microwave field from the transitions they address as shown in Fig. 1. To ensure three-photon resonance, we keep the coupling field on resonance ($\delta_c = 0$) and maintain equal detunings for the probe and microwave fields ($\delta_p = \delta_\mu$). These conditions are achieved in our system by using the same microwave source to drive the EOM and the microwave cavity. If, in addition, a two-photon resonance condition between the probe and coupling fields is satisfied, then most atoms in the

Optics EXPRESS

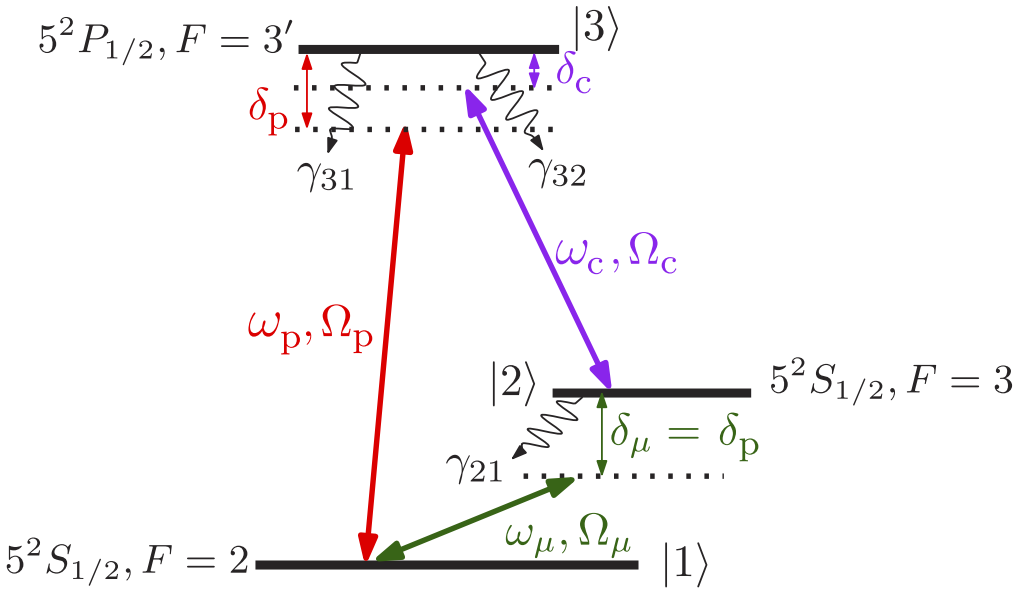

Fig. 1. A Δ configuration with hyperfine levels of ^{85}Rb D1 manifold formed by interaction with two optical fields, coupling (ω_c), probe (ω_p) and a microwave field (ω_μ).

Δ configuration will be shelved in a dark state made up of ground and meta-stable hyper-fine levels [23]. Atoms in the dark state exhibit electromagnetically induced transparency and do

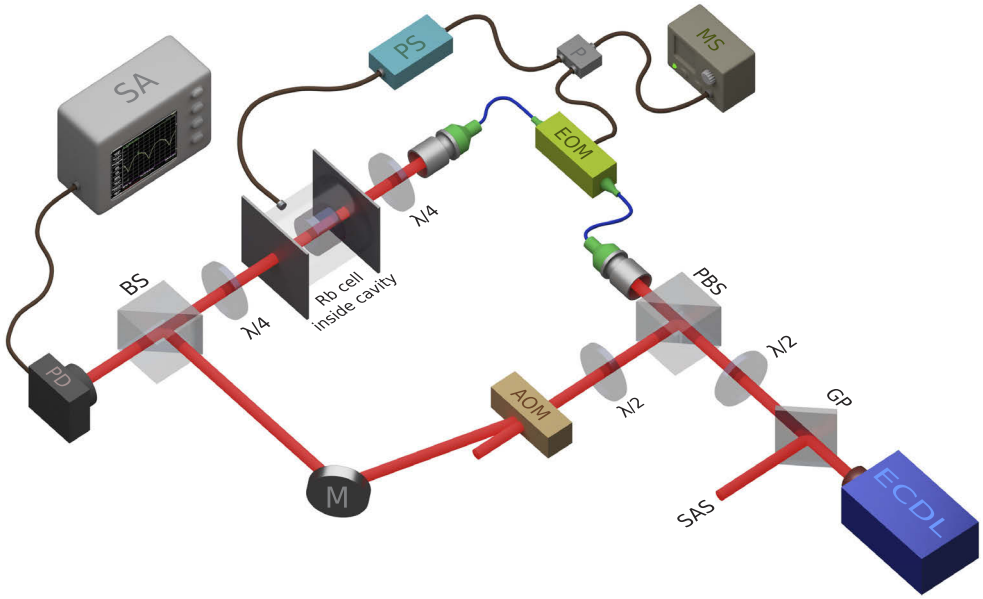

Fig. 2. Schematic of our experimental set up. Here ECDL —External Cavity Diode Laser, $\lambda/2$ —half-wave plate, $\lambda/4$ —quarter-wave plate, GP —glass plate, SAS —saturated absorption spectroscopy, PBS —polarising beam-splitter, BS —beam-splitter, M —Mirror, EOM —Electro Optic Modulator, AOM —Acousto-Optic Modulator, MS —Microwave Source, P —power splitter, PS —phase shifter, SA —Spectrum Analyser, PD —Photo-Diode.

Optics EXPRESS

not participate in linear or one-photon absorption processes. Thus, for these atoms, efficient nonlinear processes can be induced with moderate field intensities [11].

In our experiment we observe probe amplification when the microwave frequency scans around its resonance. A scan of the microwave field around the $|1\rangle \rightarrow |2\rangle$ resonance also makes the probe field to scan around the $|1\rangle \rightarrow |3\rangle$ resonance. This is because the same microwave source generates the probe field by acting on the coupling field through the EOM. Thus, once during each scan of the microwave frequency, both the two-photon and the three-photon resonance conditions for all the three fields are satisfied. In addition, because of this arrangement a relative phase between all the three fields can be unambiguously defined. Under these conditions a nonlinear three-wave mixing interaction takes place between the microwave standing wave and the beat envelope of the two optical fields. This interaction facilitates energy transfer between the cavity microwave field to the optical beat envelope resulting in probe amplification. The generated probe field adds coherently to the incident probe field for appropriate values of relative phase, which results in probe amplification. The amplified probe beam which exits the microwave cavity is separated from other co-propagating beams using a heterodyne technique and detected using a high bandwidth photo-detector and recorded in a spectrum analyzer as shown in Fig. 2.

3. Demonstration of near-ideal amplification

In a cyclically connected closed system like our Δ system, coherences and populations depend on the relative phase between all the interacting fields present in the system. The relative phase difference between the interacting fields is

$$\Delta\Phi(z) = z(k_{\mathrm{p}} - k_{\mathrm{c}}) + \phi_{\mu}. \tag{1}$$

As we see from Eq. 1, the relative phase comprises propagation phases and the phase of the microwave field. The relative phase can thus be changed either by varying the propagation phases or by changing the phase of the microwave drive field. In our experiment the relative phase has been changed by modifying the microwave-field phase in the cavity using a digital phase-shifter. Beyond a certain threshold of coupling field intensity, the probe field experiences either amplification ($G > 1$) or de-amplification ($G < 1$) depending on the relative phase $\Delta\Phi$. The nonlinear interaction leading to amplification or de-amplification arises due to a sum-frequency generation process which combines a coupling and a microwave photon to give rise to a probe photon. This nonlinear three-wave mixing process is sensitive to the phase and so, depending on the relative phase $\Delta\Phi$, we either see amplification or de-amplification. G is defined as the ratio of probe transmittance on two-photon resonance normalized with probe transmittance detuned by 1 GHz far off-resonance from the optical transition.

Figure 3 shows the variation of probe gain as a function of relative phase $\Delta\Phi$. The Δ system serves as an excellent amplifier when $\Delta\Phi = 0$ and the probe achieves a maximum gain $G_{\mathrm{max}} = 4.5$. When $\Delta\Phi = \pi$ the probe is maximally de-amplified achieving a minimum probe value $G_{\mathrm{min}} = 0.25$. Such amplification and de-amplification processes become effective with a moderate microwave intensity of 3 mW/cm^2 and a coupling intensity of 9.5 mW/cm^2.

From Fig. 3 we inferred the dependence of gain on the relative phase. In an ideal PSA, amplification occurs without adding additional noise thereby maintaining the signal to noise ratio of the output signal to be the same as that of the input signal. A conformation of a PSA working in the ideal limit is that the G_{max} and the G_{min} are related by $G_{\mathrm{min}} = \frac{1}{G_{\mathrm{max}}}$ [13].

We measured G_{max} and G_{min} values for various microwave intensities to check if our system is working as an ideal PSA as shown in Fig. 4. For low microwave intensities, we see that, as the microwave intensity increases, G_{max} also increases, and we see a corresponding decrease in G_{min} values. The G_{max} values saturate at a microwave intensity of 3 mW/cm^2. In this region, the sensitivity to G_{min} values are limited by threshold intensity of the detector which did not allow

Optics EXPRESS

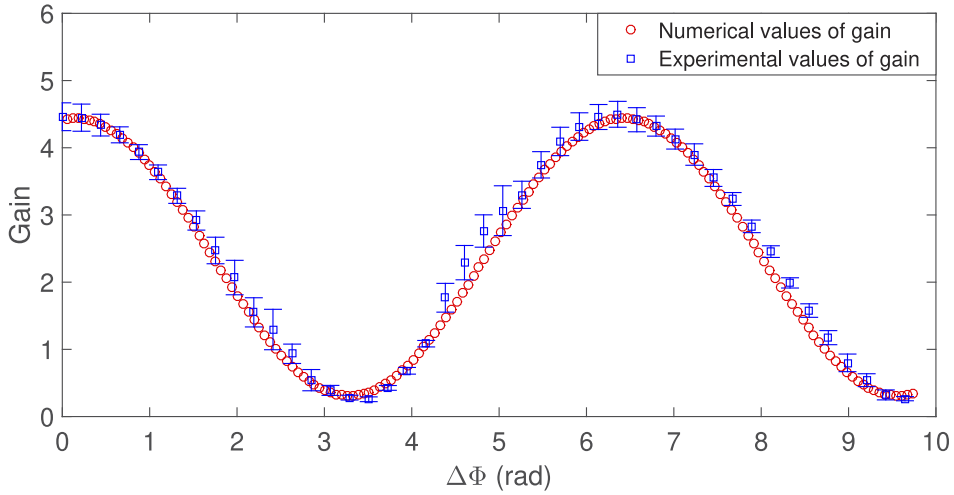

Fig. 3. Probe gain as a function of relative phase of all the three fields (ΔΦ). The phase is changed continuously using a microwave digital phase shifter. The dots are results for Gain obtained from our numerical modeling.

detection of lower $G_{\min}$ values. Within detection sensitivity we see from Fig. 4 that the measured values of $G_{\min}$ are close to $\frac{1}{G_{\max}}$ proving that our system acts like a near-ideal PSA.

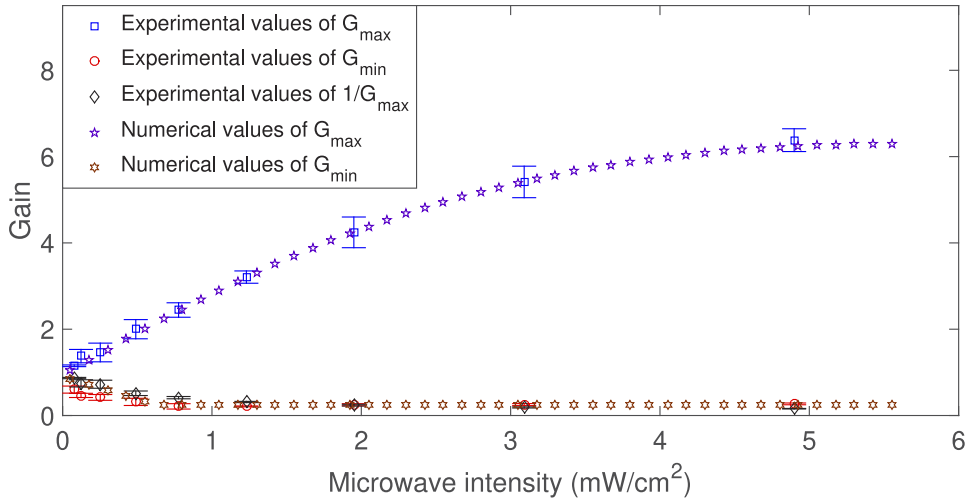

Fig. 4. Variation of maximum PSA gain ($G_{\max}$, blue square) and minimum PSA gain ($G_{\min}$, red circle) as a function of microwave intensity. For an ideal PSA $1/G_{\max}$ (black diamond) is equal to $G_{\min}$. The star points are results from our numerical calculation.

We measured the band-width of our PSA by measuring $G_{\max}$ and $G_{\min}$ values for different values of two-photon detuning $\delta := \delta_p - \delta_c$. An efficient three-wave mixing process requires a three-photon resonance condition. In our experiment we maintain three-photon resonance and measure the bandwidth of our amplifier by changing the two-photon resonance δ.

Optics EXPRESS

In Fig. 5 we plot G_{max} and G_{min} values as a function of two-photon detuning δ. In order to characterize the bandwidth of our PSA, we defined a parameter

$$C := \frac{G_{min} - \frac{1}{G_{max}}}{G_{max} - G_{min}} \tag{2}$$

which should be zero for an ideal PSA. We have chosen a cut-off value of C= 0.25 for defining the band-width of our amplification process. From Fig. 5 we see that the measured C values which are C $\leq$ 0.25 span a frequency range of approximately 500 kHz.

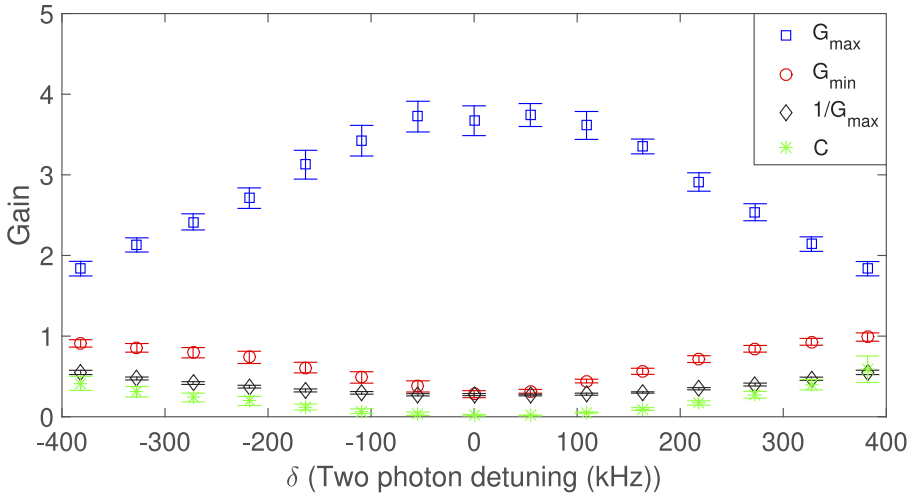

Fig. 5. Variation of G_{max} (blue square), G_{min} (red circle), $1/G_{max}$ (black diamond) and C (green star) as a function of two photon detuning for a microwave intensity of 1.2 mW/cm^2.

From Fig. 5 we can also infer that PSA occurs with maximum gain when in addition to three photon resonance, a two-photon resonance ($\delta = \delta_p - \delta_c = 0$) between the coupling and probe optical fields is also satisfied. This confirms the fact that our PSA process is a ground-state-coherence assisted PSA wherein it is the underlying formation of a EIT dark state which enables nonlinear amplification at such low light intensities, by elimination of linear absorption at line centre. The bandwidth of the optical EIT process was independently measured without the microwave field and is found to be around 800 kHz. The efficiency of our PSA process is governed by this optical EIT bandwidth.

Extinction ratio (ER) is defined as the difference between the maximum gain G_{max} and minimum gain G_{min} values of an amplifier [24,25]. A measurement of ER for fiber-optic based communication systems is of significant importance. A large ER ensures that the logical ones and zeroes are faithfully represented by high and low levels of optical signals. To test if our amplifier system has significant ER, we have calculated ER using G_{max} and G_{min} values for various values of microwave intensity. Extinction ratio values are plotted in Fig. 6. As expected, ER increases with increasing microwave intensity at lower values and saturates at around 3 mW/cm^2. The maximum ER obtained is 13 $\pm$ 0.8 dB. Our maximum extinction ratio of 13 dB obtained with a total input microwave power of 870 mW and a coupling field power of 75 μW is higher than some of the experimental fibre optical and silicon photonic crystal wave-guide demonstrations of PSA [25,26]. These experiments show a lower ER with either comparable or much higher input powers.

Optics EXPRESS

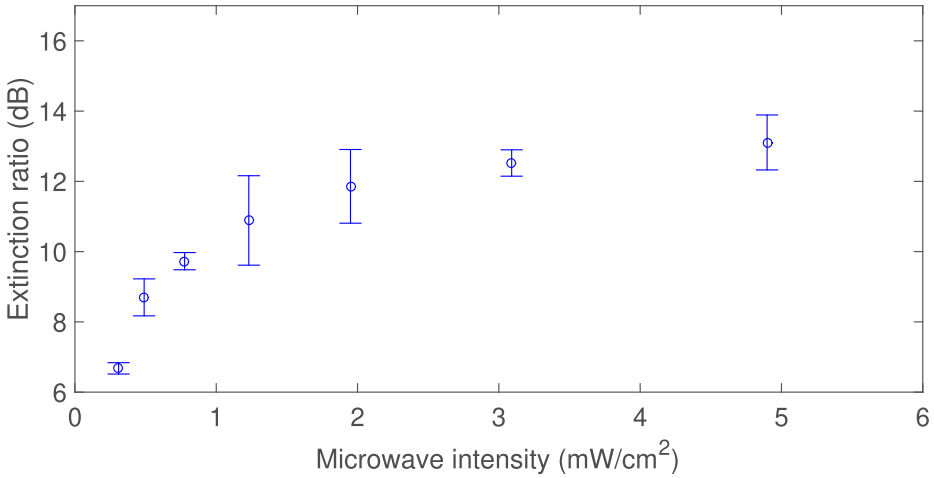

Fig. 6. Extinction ratio (ER) which is the difference between the $G_{\min}$ and $G_{\max}$ values is plotted as a function of microwave intensity.

4. Numerical modeling

In order to explain the experimental results, we have numerically modeled our Δ system. We have included exhaustively all the decay processes present in a room temperature collection of ^{85}Rb atoms with a Δ level scheme Fig. 1. This list includes the natural decay rate of the excited ($|3\rangle$) and the metastable ($|2\rangle$) states. In addition, we have included decoherence introduced by the large number of background thermal photons available at room temperature at our microwave frequency of 3.0357 GHz. We have also modelled the finite quality factor of our microwave cavity by adding a phenomenological decay constant Γ_μ.

In our numerical modeling based on [22], the optical probe and coupling fields are propagating fields through the vapor cell. Denoting the propagation direction as the z-axis, the fields are represented by

$$\boldsymbol{E}_{\mathrm{p,\,c}}(\boldsymbol{r})\cos(\omega_{\mathrm{p,\,c}}t - k_{\mathrm{p,\,c}}z + \phi_{\mathrm{p,\,c}}) \tag{3}$$

where angular frequencies $\omega_{\mathrm{p,\,c}}$, wave numbers $k_{\mathrm{p,\,c}}$ and initial phases $\phi_{\mathrm{p,\,c}}$ denote respectively the parameters of the probe and coupling fields. The microwave field is a standing wave inside our microwave cavity represented by

$$\boldsymbol{E}_\mu(\boldsymbol{r})\cos(\omega_\mu t + \phi_\mu). \tag{4}$$

We have not included the z-variation of the microwave field because in the spatial region occupied by the 1 cm length vapour cell, the microwave field remains fairly constant. Taking the reference energy level for our Hamiltonian to be the ground level $|1\rangle$, we derive the Hamiltonian of our Δ system in the interaction and rotating wave picture as

$$\begin{aligned}\hat{H}(\boldsymbol{r},\boldsymbol{v}) = \delta'_{\mathrm{p}}(\boldsymbol{v})|3\rangle\langle 3| + (\delta'_{\mathrm{p}}(\boldsymbol{v}) - \delta'_{\mathrm{c}}(\boldsymbol{v}))|2\rangle\langle 2| - \Omega_\mu(\boldsymbol{r})|1\rangle\langle 2| \\ - \Omega_{\mathrm{p}}(\boldsymbol{r})|1\rangle\langle 3| - \Omega_{\mathrm{c}}(\boldsymbol{r})|2\rangle\langle 3| + \mathrm{h.c.}\end{aligned} \tag{5}$$

with h.c. denoting Hermitian conjugate. Here

$$\delta'_{\mathrm{p}}(\boldsymbol{v}) := \delta_{\mathrm{p}} - \boldsymbol{k}_{\mathrm{p}}\cdot\boldsymbol{v}, \qquad \delta'_{\mathrm{c}}(\boldsymbol{v}) := \delta_{\mathrm{c}} - \boldsymbol{k}_{\mathrm{c}}\cdot\boldsymbol{v} \tag{6}$$

Optics EXPRESS

are Doppler-shifted detunings of the coupling and probe fields (see Fig. 1) seen by an atom moving with velocity $\boldsymbol{v}$. The complex Rabi frequencies are

$$\begin{aligned}\Omega_{\rm c}(\boldsymbol{r}) =& \boldsymbol{d}_{23}\cdot\boldsymbol{E}_{\rm c}(\boldsymbol{r}),\\ \Omega_{\rm p}(\boldsymbol{r}) =& \boldsymbol{d}_{13}\cdot\boldsymbol{E}_{\rm p}(\boldsymbol{r}),\\ \Omega_{\mu}(\boldsymbol{r}) =& \boldsymbol{\mu}_{12}\cdot\boldsymbol{B}_{\mu}(\boldsymbol{r})e^{i(\omega_{\mu}+\omega_{\rm c}-\omega_{\rm p})t+i(k_{\rm p}-k_{\rm c})z+i(\phi_{\rm c}-\phi_{\rm p}+\phi_{\mu})}.\end{aligned} \tag{7}$$

The electric- and magnetic-dipole matrix elements are represented by $\boldsymbol{d}_{\rm ij}$ and $\boldsymbol{\mu}_{\rm ij}$ respectively and $\boldsymbol{B}_{\mu}$ is the microwave magnetic field flux density. Using the dipole approximation, the Rabi frequencies of the probe, coupling, and microwave fields are taken to be spatially uniform. They are thus represented as $\Omega_{\rm c}(\boldsymbol{r})\equiv\Omega_{\rm c}$, $\Omega_{\rm p}(\boldsymbol{r})\equiv\Omega_{\rm p}$ and $\Omega_{\mu}(\boldsymbol{r})\equiv\Omega_{\mu}$. As is well known, propagation and temporal phases of EM fields in a closed-loop Δ system do not vanish in the interaction picture unlike that of a Λ system [23]. Representing the three-photon resonance condition employed in our experiment, we choose $\delta_{\rm c}=0$, and maintain $\delta_{\rm p}=\delta_{\mu}$ in our calculations, reflecting our experimental arrangement. As probe and coupling fields are generated from EOM the initial phase of both the fields are locked, we have taken this into account by keeping $\phi_{\rm c}=\phi_{\rm p}$. We explicitly include the propagation phases that give rise to an effective position-dependent microwave Rabi frequency, which is $\Omega_{\mu}(z)=\Omega_{\mu}e^{i\phi_{\mu}}e^{i(k_{\rm p}-k_{\rm c})z}$.

Dynamical evolution of density matrix elements, in the interaction picture, is given by the master equation [22]

$$\dot{\sigma}(\boldsymbol{v},\ z)=-i[\hat{H}(\boldsymbol{v},\ z),\sigma(\boldsymbol{v},\ z)]+\sum_{k=1}^{5}\mathfrak{L}(\hat{a}_k)\sigma(\boldsymbol{v},\ z) \tag{8}$$

with $\mathfrak{L}(\hat{a}_k)$ the Lindblad superoperator

$$\mathfrak{L}(\hat{a})\sigma=\hat{a}\sigma\hat{a}^{\dagger}-\frac{1}{2}\{\sigma,\hat{a}^{\dagger}\hat{a}\} \tag{9}$$

acting on operators

$$\begin{aligned}\hat{a}_1 =& \sqrt{(\bar{n}+1)\Gamma_{12}}|1\rangle\langle 2|,\\ \hat{a}_2 =& \sqrt{\bar{n}\Gamma_{12}}|2\rangle\langle 1|,\ \hat{a}_3=\sqrt{\Gamma_{13}}|1\rangle\langle 3|,\\ \hat{a}_4 =& \sqrt{\Gamma_{23}}|2\rangle\langle 3|,\\ \hat{a}_5 =& \sqrt{\Gamma_{\mu}}(|1\rangle\langle 1|-|2\rangle\langle 2|)\end{aligned} \tag{10}$$

with Γ_{12} and $\Gamma_{23}=\Gamma_{13}$ representing natural linewidths of levels $|2\rangle$ and $|3\rangle$ respectively, and Γ_{μ} being the phenomenological decay constant modeling the finite quality factor of our microwave cavity. At temperature T, $\bar{n}$ is the average number of thermal photons in the bath. Steady-state values of $\sigma(v)$ are obtained by solving Eq. (5) to Eq. (10). These solutions are then averaged over the Maxwell-Boltzmann velocity profile at a temperature T of 300 K in accordance with our experiment.

We change the relative phase of all the three fields by modifying the absolute phase value of the microwave field. In our experiment we employ a Rb vapor cell of length $L=1$ cm. The finite size of our cell is in the z-dependent phase variations of density-matrix elements. We treat the Rb cell as a sequence of small cell units along the propagation direction to simulate the changes in the probe field as it passes through our experimental cell of 1 cm length. The slowly-varying envelope approximation is used to calculate the propagation equation for the probe field in each cell, which is [27]

$$\frac{\partial\Omega_{\rm p}}{\partial z}=-i\eta\bar{\sigma}_{31}. \tag{11}$$

In this equation phase-dependent steady-state density matrix element is represented by $\bar{\sigma}_{31}$ corresponding to probe absorption, and is obtained using Eq. (5) to Eq. (10). The coupling

Optics EXPRESS

constant $\eta = \frac{d_{13}^2 \omega_p N}{2\epsilon_0 c\hbar}$. Here N is the number density of our atoms which is 10^8 atoms/cc, $d_{13}^2 = 3.57 \times 10^{-58}$ C^2m^2 and c is the speed of light. The coupling constant η has units of $m^{-1}s^{-1}$ and is taken to be to 1 representing very closely the value for η derived for our experimental parameters.

We plot numerically computed probe transmission values for various values of relative phase ($\Delta\Phi$) in Fig. 3 along with our experimentally measured values. As can be seen in this figure our computed probe transmission values agree well with the experimental values. We have also numerically calculated probe transmission values for $\Delta\Phi = 0$ and for $\Delta\Phi = \pi$ as a function of microwave intensity and given these values along with our experimental measurements in Fig. 4. As can be seen the computed results are in very good agreement with experimentally measured values. In our numerical calculations we have used values of field intensities very similar to our experimental values. The only free parameter used in the calculation is an overall scaling factor applied to the y-axis values to match with the experimental measurements.

5. Significance of our experimental results

Phase-sensitive amplification has been experimentally demonstrated using a three wave mixing ($\chi^{(2)}$) process earlier using classical nonlinear crystals [13]. In alkali atomic vapours possessing ground state coherence, all previous demonstrations of PSA used a four-wave mixing ($\chi^{(3)}$) nonlinear interaction [18,25]. In most demonstrations, the interacting fields are within a narrow band-width of frequencies and amplification is seen in an all-optical domain. Our experimental demonstration of a near-ideal PSA where amplification is demonstrated in an optical field by controlling parameters of a microwave field is the first of its kind across various physical systems.

Our hydrid-PSA spanning electromagnetic fields, which are several orders apart in frequency, is of immense practical interest. In particular our PSA between microwave and optical fields can be used to obtain radio-over-fiber implementations for coherent amplification of classical signals. It is to be noted that a Rydberg atom based optical communication protocol interfacing with a fiber-optic link for transmission of RF signals has already been demonstrated [28]. Such communication protocols can readily be implemented with our system with the added advantage of high amplification and good extinction ratio.

More importantly, if our scheme is implemented with cold atoms, it can readily serve as an ideal interface for coherent transfer and amplification of quantum signals created in the microwave domain [29] to the optical domain. The amplification which will be obtained with such ultra-cold atoms will be several fold higher as was explicitly calculated in our earlier publication [22]

Low-field-few-atom nonlinearity is a desirable goal [30] for design of quantum logic gates. In this experiment we demonstrated nonlinear amplification of the probe with very low optical densities of our Rb vapour, achieving a high gain of 7 dB with an optical density 0.45. This is one of the lowest density nonlinearities demonstrated amongst atomic vapours showing PSA [18,19] and the first such low density demonstration in a hybrid architecture.

6. Conclusion

We experimentally achieve phase-sensitive amplification (PSA) in a dilute sample of ^{85}Rb atoms using a hybrid three-wave mixing process connecting microwave and optical frequencies. This is the first demonstration of PSA working across frequency regimes that are separated by several orders. We observe amplification with atoms shelved in a long-lived dark state even at very low optical densities. We have shown that our system operates as a near-ideal PSA with a bandwidth of 500 kHz. This opens the possibility of achieving quantum noise-limited signal transfer across widely separated frequency regimes.

Optics EXPRESS

Funding

Department of Science and Technology, Government of India.

Acknowledgments

BCS acknowledges the VAJRA scheme of SERB, department of science and technology, India for their support. AK, AKV, PKN and AN thank Pascal Neveu of Laboratoire Aimé Cotton for useful discussions and Meena M S, Somashekar R, Arsalan Md and Ibrahim M of Raman Research Institute for their technical support.

References

1. R. C. Pooser, A. M. Marino, V. Boyer, K. M. Jones, and P. D. Lett, "Low-noise amplification of a continuous-variable quantum state," Phys. Rev. Lett. **103**(1), 010501 (2009).
2. Z. Qin, L. Cao, H. Wang, A. M. Marino, W. Zhang, and J. Jing, "Experimental generation of multiple quantum correlated beams from hot rubidium vapor," Phys. Rev. Lett. **113**(2), 023602 (2014).
3. V. Boyer, A. M. Marino, and P. D. Lett, "Generation of spatially broadband twin beams for quantum imaging," Phys. Rev. Lett. **100**(14), 143601 (2008).
4. S. Kim and A. M. Marino, "Generation of ^{87}Rb resonant bright two-mode squeezed light with four-wave mixing," Opt. Express **26**(25), 33366–33375 (2018).
5. G. Alzetta, A. Gozzini, L. Moi, and G. Orriols, "An experimental method for the observation of r.f. transitions and laser beat resonances in oriented na vapour," Il Nuovo Cimento B (1971-1996) **36**(1), 5–20 (1976).
6. E. Arimondo and G. Orriols, "Nonabsorbing atomic coherences by coherent two-photon transitions in a three-level optical pumping," Lettere al Nuovo Cimento (1971-1985) **17**(10), 333–338 (1976).
7. H. R. Gray, R. M. Whitley, and C. R. Stroud, "Coherent trapping of atomic populations," Opt. Lett. **3**(6), 218–220 (1978).
8. K.-J. Boller, A. Imamoğlu, and S. E. Harris, "Observation of electromagnetically induced transparency," Phys. Rev. Lett. **66**(20), 2593–2596 (1991).
9. J. E. Field, K. H. Hahn, and S. E. Harris, "Observation of electromagnetically induced transparency in collisionally broadened lead vapor," Phys. Rev. Lett. **67**(22), 3062–3065 (1991).
10. M. D. Lukin, P. R. Hemmer, M. Löffler, and M. O. Scully, "Resonant enhancement of parametric processes via radiative interference and induced coherence," Phys. Rev. Lett. **81**(13), 2675–2678 (1998).
11. S. E. Harris, J. E. Field, and A. Imamoğlu, "Nonlinear optical processes using electromagnetically induced transparency," Phys. Rev. Lett. **64**(10), 1107–1110 (1990).
12. D. Wang, C. Liu, C. Xiao, J. Zhang, H. M. Alotaibi, B. C. Sanders, L.-G. Wang, and S. Zhu, "Strong coherent light amplification with double electromagnetically induced transparency coherences," Sci. Rep. **7**(1), 5796 (2017).
13. J. A. Levenson, I. Abram, T. Rivera, and P. Grangier, "Reduction of quantum noise in optical parametric amplification," J. Opt. Soc. Am. B **10**(11), 2233–2238 (1993).
14. J. A. Levenson, I. Abram, T. Rivera, P. Fayolle, J. C. Garreau, and P. Grangier, "Quantum optical cloning amplifier," Phys. Rev. Lett. **70**(3), 267–270 (1993).
15. T. Li, B. E. Anderson, T. Horrom, B. L. Schmittberger, K. M. Jones, and P. D. Lett, "Improved measurement of two-mode quantum correlations using a phase-sensitive amplifier," Opt. Express **25**(18), 21301–21311 (2017).
16. C. Jiang, L. N. Song, and Y. Li, "Directional phase-sensitive amplifier between microwave and optical photons," Phys. Rev. A **99**(2), 023823 (2019).
17. A. M. Akulshin, R. J. McLean, A. I. Sidorov, and P. Hannaford, "Coherent and collimated blue light generated by four-wave mixing in Rb vapour," Opt. Express **17**(25), 22861–22870 (2009).
18. N. V. Corzo, A. M. Marino, K. M. Jones, and P. D. Lett, "Noiseless optical amplifier operating on hundreds of spatial modes," Phys. Rev. Lett. **109**(4), 043602 (2012).
19. P. Neveu, C. Banerjee, J. Lugani, F. Bretenaker, E. Brion, and F. Goldfarb, "Phase sensitive amplification enabled by coherent population trapping," New J. Phys. **20**(8), 083043 (2018).
20. K. V. Adwaith, A. Karigowda, C. Manwatkar, F. Bretenaker, and A. Narayanan, "Coherent microwave-to-optical conversion by three-wave mixing in a room temperature atomic system," Opt. Lett. **44**(1), 33–36 (2019).
21. M. Ghosh, A. Karigowda, A. Jayaraman, F. Bretenaker, B. C. Sanders, and A. Narayanan, "Demonstration of a high-contrast optical switching in an atomic delta system," J. Phys. B **50**(16), 165502 (2017).
22. M. Manjappa, S. S. Undurti, A. Karigowda, A. Narayanan, and B. C. Sanders, "Effects of temperature and ground-state coherence decay on enhancement and amplification in a Δ atomic system," Phys. Rev. A **90**(4), 043859 (2014).
23. S. J. Buckle, S. M. Barnett, P. L. Knight, M. A. Lauder, and D. T. Pegg, "Atomic interferometers," Opt. Acta **33**(9), 1129–1140 (1986).
24. Y. Zhang, J. Schröder, C. Husko, S. Lefrancois, D.-Y. Choi, S. Madden, B. Luther-Davies, and B. J. Eggleton, "Pump-degenerate phase-sensitive amplification in chalcogenide waveguides," J. Opt. Soc. Am. B **31**(4), 780–787 (2014).

Optics EXPRESS

25. Y. Zhang, C. Husko, J. Schröder, S. Lefrancois, I. H. Rey, T. F. Krauss, and B. J. Eggleton, "Phase-sensitive amplification in silicon photonic crystal waveguides," Opt. Lett. **39**(2), 363–366 (2014).
26. X. Fu, X. Guo, and S. Chester, "Raman-enhanced phase-sensitive fibre optical parametric amplifier," Sci. Rep. **6**(1), 20180 (2016).
27. H. Li, V. A. Sautenkov, Y. V. Rostovtsev, G. R. Welch, P. R. Hemmer, and M. O. Scully, "Electromagnetically induced transparency controlled by a microwave field," Phys. Rev. A **80**(2), 023820 (2009).
28. A. B. Deb and N. Kjaergaard, "Radio-over-fiber using an optical antenna based on rydberg states of atoms," Appl. Phys. Lett. **112**(21), 211106 (2018).
29. G. Wendin, "Quantum information processing with superconducting circuits: a review," Rep. Prog. Phys. **80**(10), 106001 (2017).
30. A. Javadi, I. Söllner, M. Arcari, S. L. Hansen, L. Midolo, S. Mahmoodian, G. Kiršanskė, T. Pregnolato, E. Lee, J. Song, S. Stobbe, P. Lodahl, and J. Song, "Single-photon non-linear optics with a quantum dot in a waveguide," Nat. Commun. **6**(1), 8655 (2015).